Numerical calculation of soil water potential in an irrigated 'conference' pear orchard

Pieter Janssens [a,*], Jan Diels [b], Jan Vanderborght [b,c], Frank Elsen [a],
Annemie Elsen [a], Tom Deckers [d], Hilde Vandendriessche [a,e]

[a] Soil Service of Belgium, W. de Croylaan 48 B-3001 Heverlee, Belgium
[b] Katholieke Universiteit Leuven Division of Soil and Water Management, Celestijnenlaan 200e - bus 2411 B-3001 Leuven, Belgium
[c] Forschungszentrum Jülich GmbH Agrosphere, IBG-3 D-52425 Jülich, Germany
[d] PCFruit Research Station Fruittuinweg 1 B-3800 Sint-Truiden (Kerkom), Belgium
[e] Katholieke Universiteit Leuven Division of Crop Biotechnics W. De Croylaan 48 B-3001 Leuven, Belgium

ARTICLE INFO

ABSTRACT

Irrigation in Belgian 'Conference' pear orchards is often managed by soil water potential (Ψ_{soil}) sensors. The most widespread sensor among fruit growers in Belgium is the Watermark sensor (Irrometer Co., USA). To gain better insight into the use of the Watermark soil sensor for irrigation scheduling in pear orchards the water extraction pattern of the 'Conference' pear trees was acquired by a numerical calculation of Ψ_{soil} in three experimental plots. A reasonable accordance between calculated and measured Ψ_{soil} was observed with $R^2 = 0.56$ and RMSE = 13.4 kPa over 1320 observations. Furthermore the sensitivity of the numerical calculation to the selected root distribution was shown. The Ψ_{soil} calculation with the root distribution parameterized by site specific fine root length observations gave satisfactory results for all plots, in contrast to Ψ_{soil} calculation based on other root distributions.

© 2014 Elsevier B.V. All rights reserved.

1. Introduction

In Belgium 'Conference' pear tree (*Pyrus Communis*, cv. 'Conference') is irrigated to maintain a high fruit yield in dry years (Janssens et al., 2011). Belgium is situated in the temperate climate zone with a relatively low average evapotranspiration and a high but variable rainfall from bloom (first half of April) to harvest (first half of September). Irrigation in the orchards is supplied by drip irrigation on a weed free strip under the canopy of the trees. Irrigation scheduling in the orchards is often managed by soil water potential (Ψ_{soil}) sensors. The sensor the most widespread among fruit growers in Belgium is the Watermark sensor (Irrometer Co., USA). This sensor is an electrical resistance sensor with two electrodes embedded in a granular matrix. The granular matrix is a gypsum tablet increased in polyvinyl chloride plastic fill. The use of the sensor entails some limitations (Scanlon et al., 2002): The relation between water content and matrix potential in the sensor is hysteric (Bourget et al., 1958; Whaylley et al., 2001); errors may occur during rapid drying or rewetting of the soil (McCan et al., 1992) and the maximal pressure head that can be measured is −10 kPa which is the air entry pressure value of the sensor. Errors due to the hysteric response of the sensor can be minimized by calibration based on the specific drying or wetting curves form the soil or by creating a sensor with a ceramic-based porous matrix (Whaylley et al., 2001). A comparative study between various soil moisture sensors indicates that the accuracy of the sensor is comparable to the widely spread frequency domain reflectometer (FDR), time domain reflectometer (TDR) and gypsum block but lower than the neutron probe (Leib et al., 2003). Due to the low cost and ease of operation the Watermark sensors are useful as a qualitative indicator for matrix potential and therefore suitable for irrigation scheduling on commercial farms (Jabro et al., 2009; Thompson et al., 2006).

Since drip irrigation causes rapid and variable changes in Ψ_{soil} distribution knowledge of soil water dynamics in the root zone of pear orchards permits better insight into the use of the Watermark soil sensor. Root water extraction patterns have been calculated previously in various fruit crops e.g. apple (Arbat et al., 2008; Besharat et al., 2010; Gong et al., 2006; Green and Clothier, 1999; Green et al., 2003) almond (Phogat et al., 2012; Vrugt et al., 2001a,b), grape (Zhou et al., 2007), orange (Consoli et al., 2014) and pear (Yao et al., 2011). In almost all these studies the numerical calculations have been compared with FDR, TDR or neutron probe recordings of soil water content. The question remains to what extent Ψ_{soil} observations, achieved with Watermarks

sensors, can be related to numerical calculations of water extraction patterns.

Root water uptake patterns of trees can be calculated numerically using a sink term presented by Feddes et al. (1978). This sink term includes functions which account for crop transpiration, response to water stress and the root distribution of the crop:

$$\frac{\partial \theta}{\partial t} = \frac{\partial}{\partial x}\left[K(h)\left(\frac{\partial h}{\partial x}\right)\right] + \frac{\partial}{\partial z}\left[K(h)\left(\frac{\partial h}{\partial z}\right) - K(h)\right] - S(x, z, t)$$
(1)

$$S(x, z, t) = T_p\beta(x, z)\alpha(h, x, z)$$
(2)

where, θ is the volumetric water content, h (m) is hydraulic head, t is the time, x, z is the position, K (m d^{-1}) is the hydraulic conductivity. S (d^{-1}) is the sink term depending on potential transpiration rate (T_p) (m d^{-1}), a normalized root distribution function $\beta(x, z)$ (m^{-1}) and a dimensionless water stress response function $\alpha(h, x, z)$.

The numerical calculation of Eq. (1) can be executed with HYDRUS (Simunek et al., 2006). HYDRUS is designed to describe water movement in the vadose zone and has a broad range of applications. HYDRUS is often used to study irrigation design and root water uptake patterns (Arbat et al., 2008; Phogat et al., 2012; Vrugt et al., 2001a,b; Yao et al., 2011; Zhou et al., 2007). Input parameters needed for the numerical calculation are soil hydraulic properties, rainfall, irrigation rate, evaporation, transpiration of the tree and root distribution of the tree. Soil hydraulic properties, $\theta(h)$ and $K(h)$ relationships, can be measured in the field, laboratory or derived from pedotransferfunctions such as ROSETTA (Schaap et al., 2001) which is embedded in the HYDRUS software. Rocha et al. (2006) pointed out that especially the shape of the water retention curve, θ_{sat} and K_{sat} have a big influence on the HYDRUS calculation. Rainfall and irrigation can be measured on site, transpiration of the tree can be measured by sap flow gauges or derived from reference evapotranspiration (ET$_o$) with crop coefficients (Allen et al., 1998). Root distribution of the tree is probably one of the parameters that is the most difficult to obtain. In this case root distribution may be crucial since it can be expected to play a major role in the water extraction pattern of the tree. Previously root distributions for numerical calculations have been derived from observed root length densities (Gong et al., 2006; Green and Clothier, 1999; Green et al., 2003; Yao et al., 2011; Zhou et al., 2007), derived from literature (Phogat et al., 2012), assumed to decrease linearly with depth (Arbat et al., 2008) or derived from soil moisture observations using inverse modelling techniques (Besharat et al., 2010; Vrugt et al., 2001a,b). This raises the question which procedure is most suited for a reliable calculation of Ψ_{soil} distribution in the Conference pear orchards.

First objective of this study is to evaluate to what extent Ψ_{soil} observations obtained with Watermark sensors in irrigated pear orchards can be related to numerical calculations of Ψ_{soil} distribution. Secondly the sensitivity of the HYDRUS calculation to the implemented root distribution is investigated.

2. Materials and methods

2.1. Plant material and site description

The experiment was conducted in an orchard planted with Conference pear trees on a Quince Adams rootstock, situated in Belgium, Sint-Truiden (50°45′59.46″N, 5° 9′24.68″E). Belgium is situated in a temperate climate zone with frequent rainfall events and a relatively low evapotranspiration during the growing season. Average rainfall in Belgium during the growing season from April to August is 67 mm/month, average reference evapotranspiration

(ET$_o$) is 85 mm/month. However in 48% of the years between 1959 and 2012, rain deficits of 60 mm/month occurred. The trees were planted in 1996 with a planting distance of 3.5 m by 1.5 m. The average tree height was 3.5 m. The trees were trained in a free spindle system. The orchard was situated on a uniform silt loam textured soil. The organic carbon content in the upper soil layer (0–23 cm) was 1.1%. Rainfall was recorded on site; ET$_o$ was calculated using the Penman–Montheith equation (Allen et al., 1998) based on data recorded in a regional weather station at 20 km from the site. In the orchard a drip irrigation system was installed with line drippers every 20 cm with a discharge rate of 2 L/h. Distance between the line drippers and the trunk was 35 cm. Management practices such as pruning, disease control, fertilization and mulching were carried out in the same way as in a commercial orchard. The EC of the irrigation water was 0.87 dS m^{-1} at 25 °C.

2.2. Soil water potential (Ψ_{soil}) observations

Three plots (plot A, B and C) in the centre of the orchard were selected for the experiment. Every plot consisted of four trees with in the centre one tree around which Watermark sensors were installed (Fig. 1). Sensors were installed on six positions perpendicular to the tree line. The numerical Ψ_{soil} calculations were executed in 2D in the plane XZ, with X being the horizontal coordinate perpendicular to the tree line and Z being the vertical coordinate. The calculation of Ψ_{soil} in 2D is a simplification of the reality but was done to ease the computation time. Previously the calculation of water distribution after drip irrigation, with the drippers in line, has been calculated successfully in 2D in a plane perpendicular to the drip line (Skaggs et al., 2004; Zhou et al., 2007). All sensors were installed at a depth of 30 cm in search of a gradient in Ψ_{soil} independent from suction due to gravity. It is expected that root concentration is highest in the soil layers close to 30 cm depth. Installing more sensors in the root zone would possibly disturb the soil too much for a representative experiment. To supply information on water content in the deeper soil layers gravimetric soil moisture samples were taken at a depth of 30–60 cm, at reasonable distance from the sensors to prevent further soil disturbance. The Watermark sensors were connected to a data logger which recorded Ψ_{soil} every 4 h. The standard manufacturer calibration was used to compute Ψ_{soil} from the electrical resistance measured by the sensors. In every plot the sensors were brand new and used for the first time. Sensors were installed 1 day before the start of the observation period according to manufactory guidelines. In plot A Ψ_{soil} was recorded in 2009 while in plot B and C Ψ_{soil} was recorded in 2011. In the irrigated plots irrigation was scheduled using the Watermark sensors. Irrigation was initiated when Ψ_{soil} decreased to −40 kPa, the irrigation dose ranged between 1 and 3 mm/day.

2.2.1.1. Plot A Ψ_{soil} observed in 2009 in an irrigated plot
In plot A Ψ_{soil} was observed between 04/06/2009 and 15/08/2009. Sensors were only installed at positions 2, 3, 4 and 5 according to Fig. 1. Total irrigation amount during this period was 77 mm, 132 mm rainfall was recorded and total ET$_o$ during this period was 255 mm.

2.2.1.2. Plot B Ψ_{soil} observed in 2011 in an irrigated plot
In plot B Ψ_{soil} was observed between 20/04/2011 and 15/07/2011. Sensors were installed at positions 1, 2, 3, 4, 5 and 6 according to Fig. 1. Total irrigation amount during this period was 45 mm, 112 mm rainfall was recorded and total ET$_o$ during this period was 300 mm.

2.2.1.3. Plot C Ψsoil observed in 2011 in a non irrigated plot
Similar to plot B Ψ_{soil} was observed between 20/04/2011 and 15/07/2011. Sensors were installed at positions 1, 2, 3, 4,
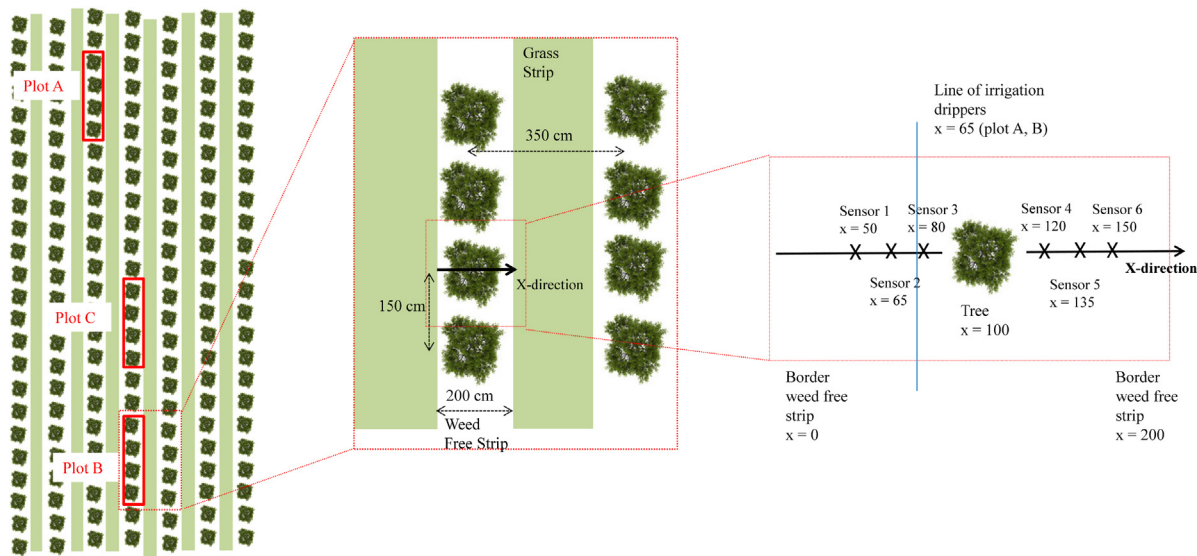
Fig. 1. Schematic top view with positions of the Watermark sensors which recorded Ψ_{soil} in every plot on six positions on the axis perpendicular to the tree line at a depth of 30 cm.

5 and 6 according to Fig. 1. In this period 112 mm rainfall was recorded and total ET_o during this period was 300 mm. In plot C no irrigation was supplied to assure lower Ψ_{soil} values in one of the three experimental plots.

2.3. Soil water content (θ)

In plot B and C soil water content (θ) was measured on the irrigated side and the non irrigated side (Fig. 1) of the trees with gravimetric moisture samples. Samples were collected on 30/06/2011, 05/07/2011 and 12/07/2011, towards the end of the observation period. Samples were taken with a gauge auger of 30 cm in the soil layers 0–30 cm and 30–60 cm. One sample consisted of minimal eight subsamples taken randomly within the treatment in the weed free strip beneath the canopy of the four trees within a plot. Gravimetric water content was measured by drying the samples at 105 °C during 24 h.

2.4. Soil hydraulic properties

The retention points were measured on pressure plates at 0, −10 kPa, −20 kPa, −31.6 kPa, −70.8 kPa, −100 kPa, −200 kPa and −1600 kPa on soil samples taken in four replications at 30 cm depth and at 60 cm depth. Saturated hydraulic conductivity (K_{sat}) was measured *in situ* in four replications with the inversed auger hole method (Kessler and Oosterbaan, 1974) and was 144 ± 24 cm day^{-1} for the soil layer 0–70 cm and 20 ± 0.1 cm day^{-1} for the soil layer 0–200 cm.

2.5. Root distribution

2.5.1. Contours of the root zone

To estimate the maximal contours of the root zone in the horizontal (X) and vertical (Z) directions, the central tree in plot A was excavated in January 2010 using low water pressure. The architecture of the coarse root system was measured in the lab with a compass, inclinometer and calliper and registered in the software ARCHIROOT (Dupuy, 2003, www.archiroot.org.uk) which translates the measurements in a multi-scale tree graph (MTG) developed by Godin and Caraglio (1998). The MTG is a multi-scale presentation of the tree, or root system and permits representation

and analysis in a grid with the plant architectural model PlantGL (Pradal et al., 2009).

2.5.2. Fine root distribution

To obtain fine root distributions cylindrical soil cores of 880 cm^3 were sampled. Roots were washed from the soil using fresh water. All roots with a diameter <2 mm were weighted with an accuracy of 0.001 g. Root length of these fine roots was determined on photographic scans of the roots with the ASSESS software (Lamari, 2002). Cores were taken at the six positions were the Watermark sensors were installed (Fig. 1) to a depth of 90 cm for plot A and to a depth of 45 cm for plot B and C. The height of the soil cores was 15 cm. In plot A 36 soil cores were taken, in plot B and C 18 cores per plot.

2.6. Numerical calculations with HYDRUS

2.6.1. Boundary conditions

An automated mesh was generated with HYDRUS 2D with boundaries such as the atmospheric boundary, free drainage boundary, no flux boundary and the variable flux boundary to account for drip irrigation (Fig. 2).
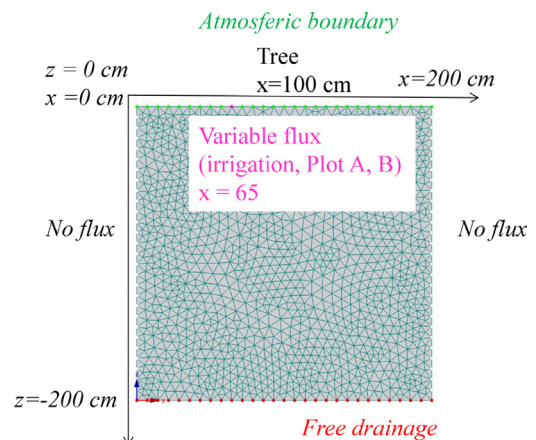
Fig. 2. Mesh generated in HYDRUS with the selected boundary conditions.

Table 1
Soil properties used in HYDRUS simulation.

Soil layers	Fitted Van Genuchten (1980) parameters						R^2	K_{sat} (cm/day)
	θ_r	θ_s	α_d (cm^{-1})	α_w (cm^{-1})	n	l		
1 (0–45 cm)	0.06	0.5	0.015	0.03	1.4	0.5	0.96	144
2 (45–75 cm)	0.09	0.43	0.01	0.02	1.4	0.5	0.91	144
3 (75–200 cm)	0.09	0.43	0.01	0.02	1.4	0.5	0.91	20

θ_r is residual water content considered at $h = -16,000$ cm $= -1600$ kPa, θ_s is saturated water content measured at $h = 0$ cm $= 0$ kPa and K_{sat} is saturated hydraulic conductivity. α_d reflects the inverse of the air-entry value during drying of the soil, α_w during wetting of the soil, n pore size distribution and l pore-connectivity (Van Genuchten, 1980).

2.6.2. Hydraulic soil properties

For establishing the $K(h)$ relationship expressed in Eq. (1) the soil hydraulic functions described by Van Genuchten (1980) were used as implemented in HYDRUS:

$$\theta(h) = \theta_r + \frac{\theta_s - \theta_r}{[1|\alpha h|^n]^m} \quad \text{when } h < 0 \quad \text{and} \quad \theta_s \quad \text{when } h \geq 0 \qquad (3)$$

$$K(h) = K_s S_e^1 \left[1 - \left(S_e^{1/m}\right)^m\right]^2 \quad \text{when } m = 1 - \frac{1}{n} \quad \text{and} \quad S_e = \frac{\theta - \theta_r}{\theta_s - \theta_r} \qquad (4)$$

where, S_e is the effective water content, θ_r residual water content considered at $h = -16000$ cm $= -1600$ kPa, θ_s saturated water content measured at $h = 0$ cm $= 0$ kPa and K_{sat} (cm/day) is saturated hydraulic conductivity. The parameters α and n according to Van Genuchten (1980), necessary for the HYDRUS calculation, were fitted through measured water retention points (Table 1; Fig. 3a). In the simulations hysteresis was considered and the wetting curve differed from the drying curve, α_w from the wetting curve equaled two times α_d from the drying curve after Kool and Parker (1987).

2.6.3. Evapotranspiration

Evaporation and transpiration was combined in the calculation as evapotranspiration (ET). Evapotranspiration (ET$_c$) of the tree was estimated with the crop specific K_c factor and ET$_o$ (Allen et al., 1998).

$$ET_c = K_c ET_o \qquad (5)$$

The K_c factor was assumed to be 1.06 times higher than that measured by Girona et al. (2004) (Fig. 3b) who obtained a 'Conference' pear tree K_c factor in a lysimeter in an orchard planted where distance between the trees in the row was 1.06 lower than the orchard in Sint-Truiden. This assumption was made due to the lack of actual measurements of light interception. The water stress response reduction function, $\alpha(h)$ in Eq. (2), used in the study is described by Feddes et al. (1978) as implemented in HYDRUS:

$$\alpha(h) = \begin{cases} \dfrac{h - h_4}{h_3 - h_4} & \text{when } h_3 > h > h_4 \\ 1 & \text{when } h_2 \geq h \geq h_3 \\ \dfrac{h - h_1}{h_2 - h_1} & \text{when } h_1 > h > h_2 \\ 0 & \text{when } h \leq h_4 \text{ and } h \leq h_1 \end{cases} \qquad (6)$$

where, h_1, h_2, h_3 and h_4 are four critical pressure heads for root water uptake. Eq. (6) is displayed in Fig. 3c. h_1 is water content at saturation of the soil at $h = 0$ cm $= 0$ kPa, h_4 is wilting point at $h = -16,000$ cm $= -1600$ kPa. In this study the threshold for water stress h_3 was set to -400 cm $= -40$ kPa independently from transpiration. The threshold for waterlogging h_2 was set to -10 cm $= -1$ kPa.

2.6.4. Initial conditions

Initial conditions were calculated with HYDRUS for a simulation period prior to the Ψ_{soil} observation period. Ψ_{soil} was calculated between 01/04/2009 and 03/06/2009 prior to the Ψ_{soil} observations in plot A. Ψ_{soil} was calculated between 01/04/2011 and 19/04/2011 prior to the Ψ_{soil} observations in plot B and C. On April 1st the soil was assumed to be at Field Capacity, -10 kPa, over the entire flow domain. April 1st can be considered as the end of winter in Belgium and the beginning of 'Conference' pear transpiration.

2.6.5. Root distribution

The normalized root distribution $\beta(x, z)$ can in HYDRUS be described by the following function proposed by Vrugt et al. (2001a):

$$\beta(x, y) = \left[1 - \frac{x}{x_m}\right] \left[1 - \frac{z}{z_m}\right] e^{-\left(\frac{p_x}{x_m}|x* - x| + \frac{p_z}{z_m}|z* - z|\right)} \qquad (7)$$

where, x_m (m), z_m (m) maximum rooting depths in the X- and Z-direction, x and z are distances from the origin in the X- and Z-direction. p_x, p_z, x^* and z^* are empirical parameters.

Maximum rooting depths (x_m and z_m) were for all plots derived from the coarse root excavation and the RLD observations to -90 cm in plot A. Maximal rooting length in X-direction (x_m) was assumed 2 m and maximal rooting depth in Z (z_m) direction was assumed 0.9 m. For each plot the empirical parameters p_x, p_z, x^* and z^* were first parameterized based on the observations of root length density of the fine roots (cm/cm^3) (RLD). Next the function was parameterized based on the observations of root weight density (g/cm^3) (RWD). Thirdly the function was parameterized based on two root distributions found in literature. Root observations in literature for pear tree are scarce but root distribution of apple was sampled by various authors. Gong et al. (2006) documented RLD observations for a 7 year old apple tree on a loam soil. Besharat et al. (2010) documented RLD observations for a 6 year old apple tree on a clay loam soil. Both root distributions were used to parameterize root density in the present Ψ_{soil} calculations.

This way four Ψ_{soil} calculations per plot where executed: (1) Ψ_{soil} calculated with $\beta(x, z)$ based on observed RLD, (2) Ψ_{soil} calculated with $\beta(x, z)$ based on observed RWD, (3) Ψ_{soil} calculated with $\beta(x, z)$ based on RLD observations of Gong et al. (2006) and (4) Ψ_{soil} calculated with $\beta(x, z)$ based on root RLD observations of Besharat et al. (2010). Purpose of the four simulations was to evaluate to what extent an in situ observation of root distribution contributes to a good calculation of Ψ_{soil} which was one of the objectives of the study.

2.6.6. Comparison between observation and calculation

Each Ψ_{soil} calculation in the flow domain was registered with six observation nodes placed at the location of the Watermark Ψ_{soil} sensors. The average daily output of the Watermark sensor was compared with the average daily Ψ_{soil} calculated on the corresponding observation node. The coefficient of determination (R^2) and the root mean square error (RMSE) were used to quantify the quality of the simulation.
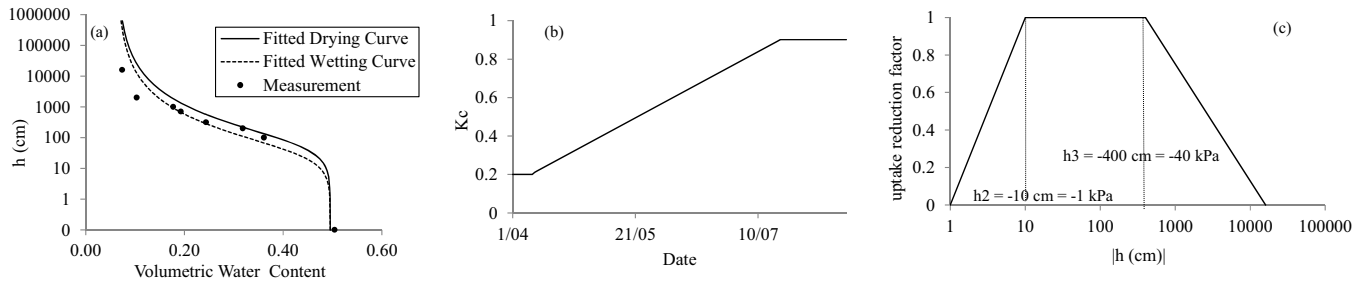
Fig. 3. The fitted drying and wetting curve using Van Genuchten (1980) for the soil layer (0–30 cm) (a), the crop factor (K_c) derived from Girona et al. (2004) which relates reference evapotranspiration (ET$_o$) to maximal crop evapotranspiration (ET$_c$) (b) and the water stress response function as used by Feddes et al. (1978) and as used in the calculation of Ψ_{soil} (c).

Besides Ψ_{soil} also average θ in the flow domain was calculated in the time steps when θ was measured. Average θ and observed θ was compared for the soil layers 0–30 cm and 30–60 cm.

2.7. Plant water status

Plant water status was recorded in plot B and C on three trees per plot by measurements of sap flow and stem water potential (Ψ_{stem}). Objective was to observe possible water stress in the non irrigated plot C and to see whether it was reflected in the HYDRUS calculation of root water uptake.

2.7.1. Sap flow

Sap flow was monitored with thermal dissipation (TD) probes. Two needles of 2 mm diameter and 20 mm long were inserted in the trunk 10 cm apart. The upper probe was heated with a constant power of 0.2 W. Based on the temperature difference between the two needles sap flux density (J_p, m^3 m^{-2} s^{-1}) was calculated

according to Granier (1985) who derived an empirical relationship between J_p and a dimensionless flow index K.

$$J_p = 0.0119 \ K^{1.1231} 360 \tag{8}$$

$$K = \frac{\Delta T_0 - T}{\Delta T} \tag{9}$$

where, ΔT is temperature difference between the two needles, ΔT_o is the temperature difference under zero flow conditions which was taken as the temperature difference at night.

Sap flow observations using the TD technique cannot be considered as an absolute estimate of sap flow or sap flux density (Gonzalez-Altozano et al., 2008; Steppe et al., 2008). The major drawbacks of the technique are that Eq. (9) is an empirical relationship which can differ between tree species. Furthermore the basic assumptions using this technique are debatable: uniform sap flow in the entire conducting sap wood area, zero sap flow at night and no vertical temperature gradient. Consequently water stress can only be detected by comparing a well irrigated plot, in this
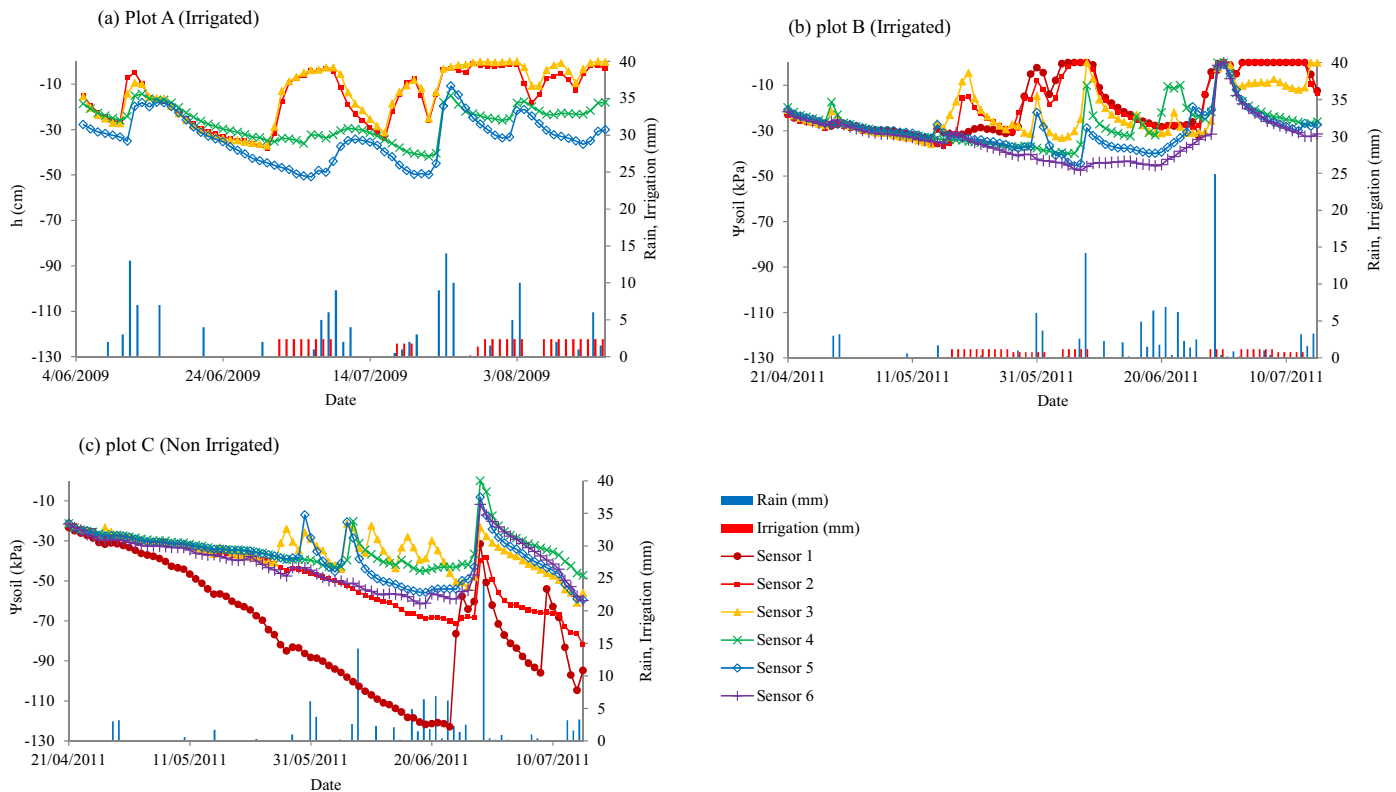
Fig. 4. Rainfall, irrigation and Ψ_{soil} observations with Watermark sensors at a depth of 30 cm in plot A (a), plot B (b) and plot C (c). Position of the sensors is outlined in Fig. 1.
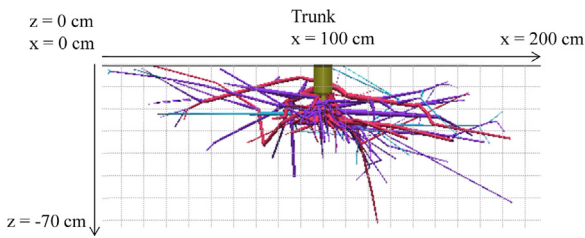
Fig. 5. Schematic of coarse roots of the tree in plot A obtained after excavation of the tree. Root architecture was measured in the lab with a compass, inclinometer and calliper and registered in the software ARCHIROOT (Dupuy, 2003).

case plot B, with less irrigated plot, in this case plot C. According to Fernandez et al. (2008) this approach leads to satisfactory water stress observations.

2.7.2. Stem water potential (Ψ_{stem})

On three trees in plot B and C Ψ_{stem} measurements were carried out on 06/05/2011, 24/05/2011, 30/06/20111 and 08/07/2011 on sunny days without rainfall. For each measurement three leaves per tree were selected from the inner part of the canopy. While still being attached, these leaves were enclosed in plastic bags covered with aluminium foil. After 60 min, the leaves were detached and the Ψ_{stem} was determined immediately using a pressure chamber (Scholander et al., 1965). The Ψ_{stem} was only recorded on sunny days without rainfall. Measurements were performed between 13.00 h and 15.00 h.

3. Results

3.1. Ψ_{soil} and θ observations

In all plots irrigation was initiated approximately one month after the start of the observation period. During the observation periods irrigation events alternated with periods of rainfall (Fig. 4). Although observed in different years, Ψ_{soil} observations in plot A (Fig. 4a) and plot B (Fig. 4b) were quite similar. Ψ_{soil} on the irrigated side of the three (positions 1, 2 and 3) decreased to -30 kPa while on the non irrigated side (positions 4, 5 and 6) Ψ_{soil} decreased to -50 kPa. Ψ_{soil} increased rapidly to 0 kPa when irrigation was applied. In the non irrigated C plot Ψ_{soil} depleted to -70 kPa on position 2 and to -120 kPa on position 1 (Fig. 4c).
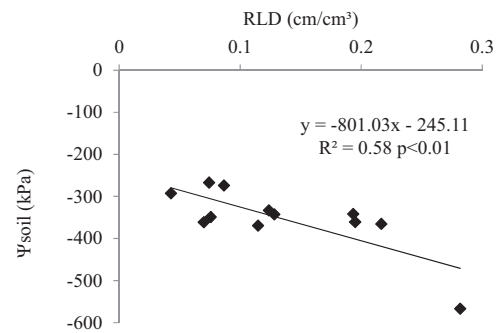

Fig. 7. Relation between Ψ_{soil} recorded with the watermark sensors on 15/05/2011 in plot B, C and RLD on the same position.

Observations of θ were correlated with the Ψ_{soil} observations. R^2 between θ sampled in the soil layer 0–30 cm and observed Ψ_{soil} was 0.80, R^2 between θ sampled in the soil layer 30–60 cm and observed Ψ_{soil} was 0.45.

3.2. Root distribution

Coarse roots of the tree excavated in plot A rooted to a depth of 70 cm and reached the borders of the weed free strip beneath the canopy (Fig. 5). Fine roots were observed to a depth of 90 cm as presented in the relative root distributions (Fig. 6a and b). Maximal fine root density in plot A was observed at a depth of 22.5 cm while in other plots maximal fine root density was observed just beneath the soil surface (Fig. 6c, d, e, f). Maximal fine root density was not always observed close to tree. RLD was for plot B and C higher at 35 cm and 50 cm from the trunk. In plot A there was a good correspondence between RLD and RWD, R^2 between both was 0.52. In plot B and plot C accordance was only moderate with R^2 being 0.20 and 0.19 respectively. Root distributions derived from literature showed the highest RLD close to the tree (Fig. 6g). Distribution in the Z-direction was similar to the observations in plot B and C (Fig. 6h).

It was possible to fit the root distribution function $\beta(x,z)$, suggested by Vrugt et al. (2001a) Eq. (7), through the fine root observations (Table 2). For all plots the quality of the fit was satisfying with R^2 0.70 or higher. Only for plots A and C the R^2 of the fit through the observed RLD was lower in the X-direction. In the
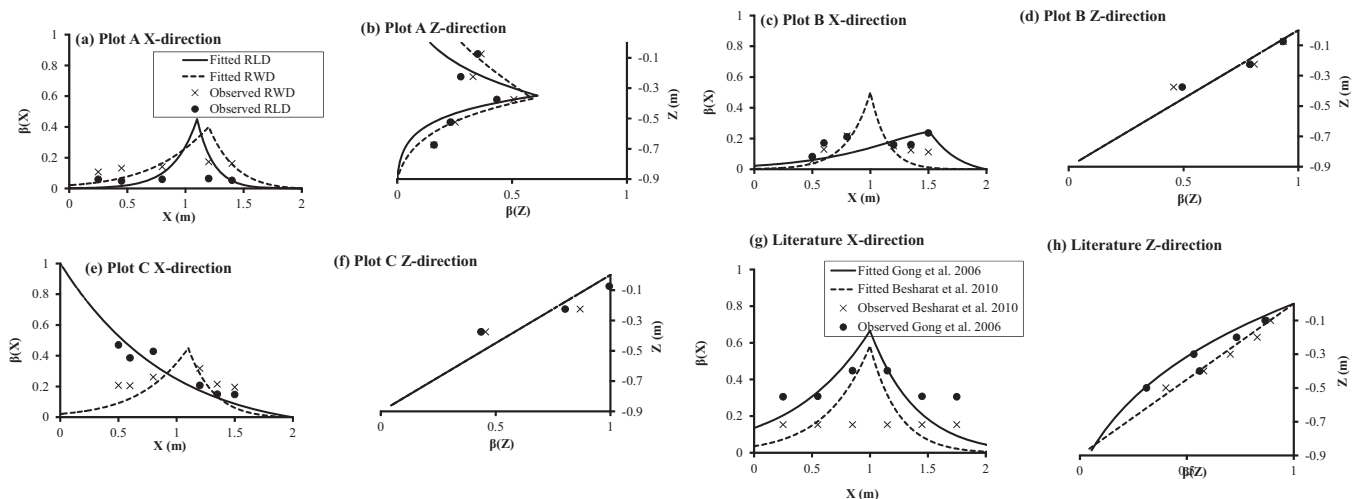
Fig. 6. Root distributions $\beta(x,z)$ used in the HYDRUS calculations. $\beta(x,z)$ was fitted using the equations suggested by Vrugt et al. (2001a,b) through RLD and RWD observations in plot A (a, b), plot B (c, d), plot C (e, f) and through RLD observations reported in literature (g, h). Parameters of $\beta(x,z)$ according to Vrugt et al. (2001a,b) are presented in Table 2.

Table 2

Parameters that define the root distributions $\beta(x,z)$ used in the HYDRUS calculations according to Vrugt et al. (2001a,b). x_m, z_m maximum rooting depths in the X- and Z-direction, x and z are distances from the origin in the X- and Z-direction, p_x, p_z, r^* and z^* are empirical parameters, R^2: Pearson correlation coefficient between observed and fitted $\beta(x,z)$. $\beta(x,z)$ is plotted in Fig. 6.

Plot nr	Observations	Horizontal distribution				Vertical distribution			
		x_m	x^*	p_x	R^2	z_m	z^*	p_z	R^2
Plot A	RLD	2	1.1	12	0.58	0.9	0.35	5	0.69
	RWD	2	1.2	6.5	0.74	0.9	0.37	3.1	0.93
Plot B	RLD	2	1.51	5	0.27	0.9	0	0	0.92
	RWD	2	1	12	0.74	0.9	0	0	0.87
Plot C	RLD	2	0	1.4	0.90	0.9	0	0	0.97
	RWD	2	1.1	7	0.97	0.9	0	0	0.95
Literature	Gong et al. (2006)	3	1	6	0.78	1	0	1	0.95
	Besharat et al. (2010)	2.4	1	8	0.88	0.9	0	0	0.96

Table 3

Quality of the HYDRUS calculation in each plot quantified by the R^2 between observation and simulation and the RMSE expressed in kPa. The numerical calculation of Ψ_{soil} by HYDRUS was based on root distributions parameterized with Root Length Density (RLD), Root Weight Density (RWD) and root observations described in literature (Gong et al., 2006, Besharat et al., 2010).

Plot	Observed RLD		Observed RWD		Gong et al., 2006		Besharat et al., 2010	
	R^2	RMSE (kPa)	R^2	RMSE (kPa)	R^2	RMSE (kPa)	R^2	RMSE (kPa)
A	0.57	11.26	0.52	11.23	0.50	11.35	0.52	11.68
B	0.49	10.20	0.42	11.35	0.41	10.94	0.42	11.22
C	0.46	16.87	0.03	22.15	0.07	21.38	0.05	21.66

Z-direction R^2 between the fit and the observations was higher than 0.73 for all plots.

An interesting relation was observed between Ψ_{soil} recorded on 15/05/2011 in plot B and C and the corresponding RLD (Fig. 7). Between the start of the observation period and 15/05/2011 no irrigation was executed yet and rainfall was limited so that the observed variation in Ψ_{soil} reflects the water uptake pattern of the trees. No similar correlation could be observed between Ψ_{soil} and RWD.

3.3. Numerical calculations with HYDRUS

The numerical calculation of Ψ_{soil} corresponded reasonable with the Ψ_{soil} observations (Table 3). However in the non irrigated plot C a satisfying calculation of Ψ_{soil} was only possible when $\beta(x,z)$ was based on RLD. Calculation of Ψ_{soil} with $\beta(x,z)$ based on RWD or root distributions found in literature yielded large errors. In plot A and B the calculation of Ψ_{soil} was only slightly better when $\beta(x,z)$ was based on RLD compared to RWD or observations derived from literature.

Overall correlation between all Ψ_{soil} observations and the corresponding Ψ_{soil} calculations was 0.56, RMSE was 13.40 kPa (Fig. 8a)

when $\beta(x,z)$ was parameterized with RLD. Accordance between calculated and observed Ψ_{soil} was erratic when observed Ψ_{soil} ranged between −20 kPa and 0 kPa. Ψ_{soil} observed by the Watermark sensor was in this range always higher compared to Ψ_{soil} achieved by the numerical calculation. Observations of θ agreed likewise with the calculated θ (Fig. 8b), at the depth of 30–60 cm R^2 was slightly lower compared to 0–30 cm depth.

The numerical calculation showed how water was distributed in the root zone after irrigation. After a 80% ET irrigation period in plot A Ψ_{soil} increased above −20 kPa in the entire irrigated side of the tree to a depth of 70 cm (Fig. 9a and b). By applying 50% ET irrigation in plot B Ψ_{soil} increased to −20 kPa only at a distance of 15 cm from the dripper (Fig. 9c and d).

3.4. Plant water status

During the first two measurements there was no differentiation in Ψ_{stem} between plot B and C (Fig. 10a). During the last two measurements at the end of the month June and the beginning of July, when irrigation was applied in plot B, there was differentiation between the treatments. The overall lowest Ψ_{stem} was −1.36 MPa and was observed in the non irrigated plot C.
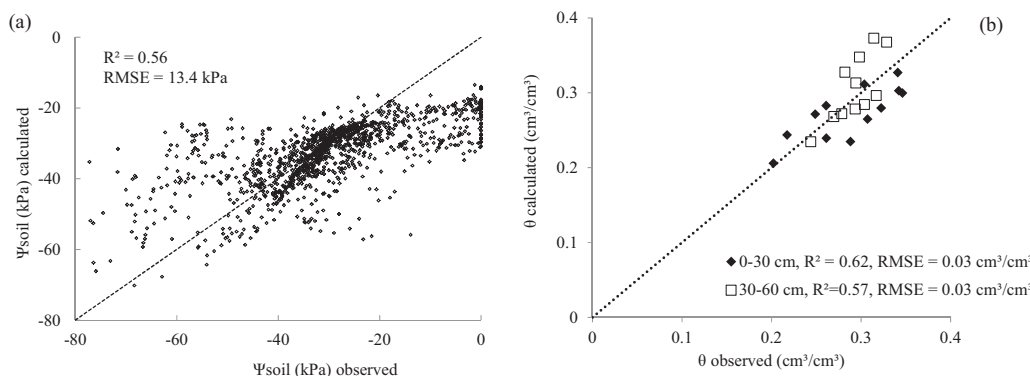
Fig. 8. Agreement between all ($n = 1320$) Ψ_{soil} observations (a) and all ($n = 24$) θ observations (b) and the corresponding numerical calculations of Ψ_{soil} and θ. Root distributions of the numerical calculations were based on RLD.
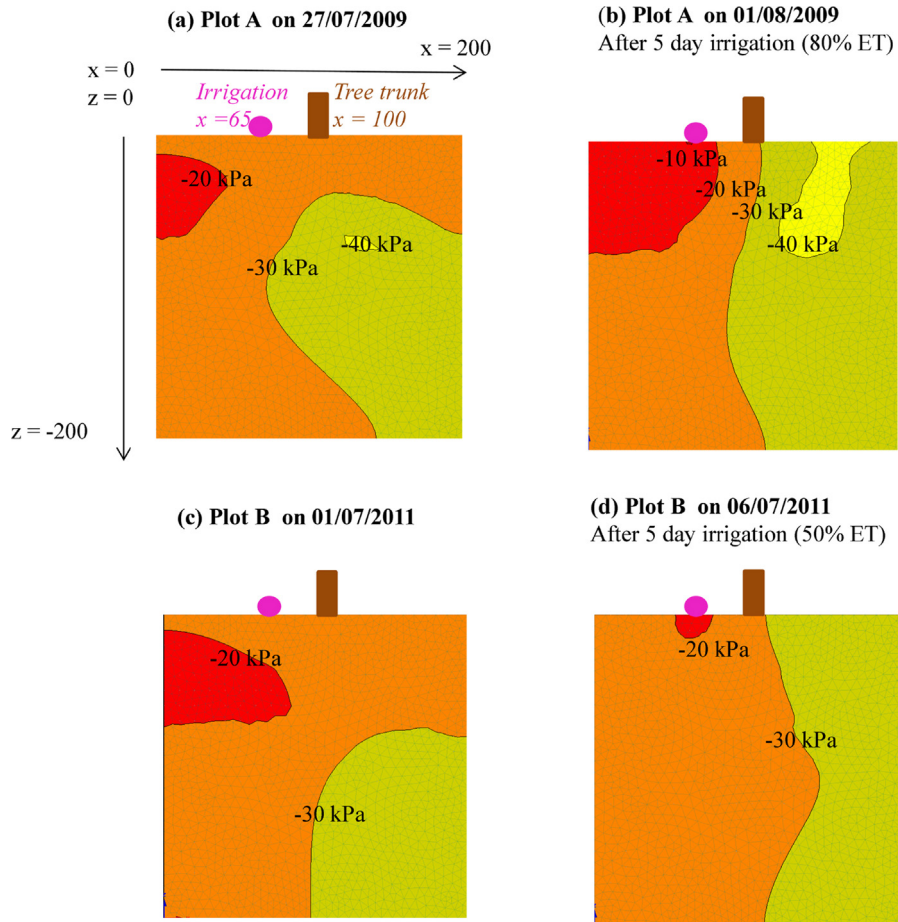
Fig. 9. Output of the Ψ_{soil} calculation in plot A on 27/07/2009 (a), 01/08/2009 (b) and plot B on 01/07/2011 (c) and 06/07/2011 (d) before and after a 5 day irrigation period of respectively 80% ET and 50% ET.
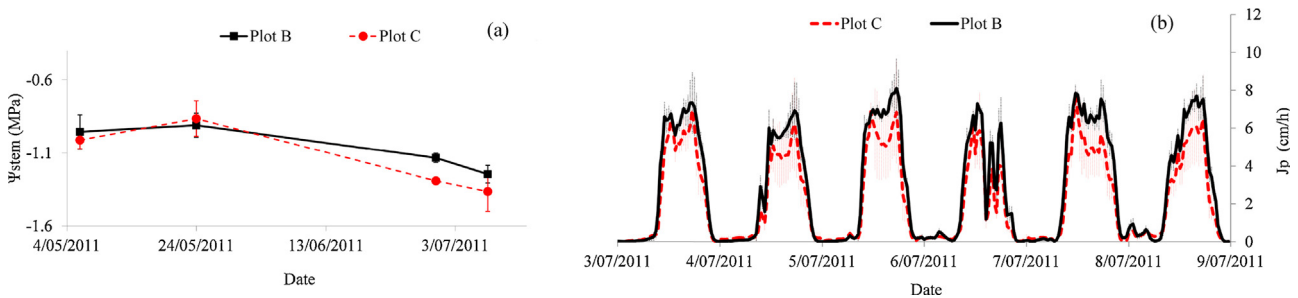

Fig. 10. Ψ_{stem} (a) and sap flux density (J_p) (b) observed in plot B and C. Vertical bars indicate standard deviation measured over three measurements per plot.
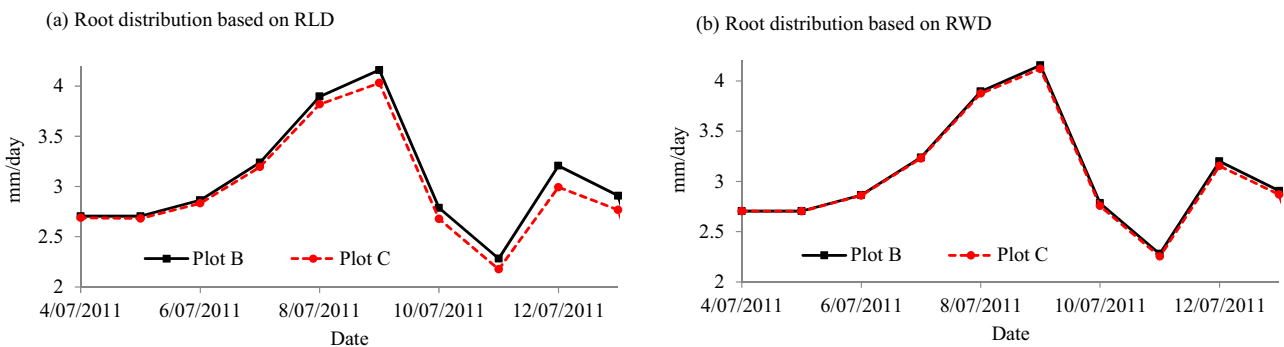

Fig. 11. Calculated root water uptake for HYDRUS calculation with root density function $\beta(x,z)$ based on RLD (a) and RWD (b).

Between 3 July and 9 July J_p tended to be lower in the non irrigated plot C compared to the irrigated plot B (Fig. 10b). The difference in J_p was only observed at noon, in the middle of the day, when evaporative demand was highest.

In the numerical calculation of root water uptake plot C differed from plot B when the root distribution function $\beta(x,z)$ was derived from RLD (Fig. 11a) but not when $\beta(x,z)$ was derived from RWD (Fig. 11b).

In general the numerical calculated Ψ_{soil} agreed reasonable with the observed Ψ_{soil} but the accordance between calculated and observed Ψ_{soil} was erratic when Ψ_{soil} was higher than -20 kPa. In one of the three plots, the non irrigated C plot, a reasonable accordance between calculated and observed Ψ_{soil} was only possible when the root distribution function $\beta(x,z)$ was parameterized based on RLD. In this plot mild effects of water stress could only be shown in the numerical calculation when $\beta(x,z)$ was parameterized using RLD. For other plots the chosen root distribution had less influence on the quality of the simulation although RLD still yielded the best results.

4. Discussion

First objective of the experiment was to evaluate the correspondence between the numerical calculated Ψ_{soil} and observed Ψ_{soil} with watermark sensors. Second objective was to investigate the sensitivity of the Ψ_{soil} calculation to the implemented root distribution. Both objectives should contribute to a better knowledge of the calculation of Ψ_{soil} patterns in 'Conference' pear orchards. This should result in more optimal placement of watermark Ψ_{soil} sensors, frequently used for irrigation scheduling in pear orchards.

4.1. Numerical calculation of Ψ_{soil}

Reported measurement variation from the Watermark sensor (Leib et al., 2003; Nolz et al., 2013) lies between 14% and 27%. The overall average Ψ_{soil} observation in this experiment was -32.5 kPa which means that 35–67% of the overall RMSE in this experiment can be allocated to measurement variation from the sensor. Possible sources of the variation in Ψ_{soil} calculation are the variability of soil hydraulic properties, efficiency of rainfall and estimations of crop transpiration.

General accordance between the calculated Ψ_{soil} and the observed Ψ_{soil} was equal to previous similar root water uptake calculations in fruit trees. Gong et al. (2006) calculated root water uptake of a mature apple tree in 2D with the root zone parameterized form root length observations. Calculated soil water distribution in the soil was compared to TDR observations of soil water content. R^2 ranged between 0.63 and 0.70 for 220 observations. In the present study overall R^2 between calculated Ψ_{soil} and observed Ψ_{soil} was 0.56 for 1320 observations. Zhou et al. (2007) calculated root water uptake of irrigated grape in 2D with HYDRUS and parameterized the root zone from root length observations. Calculated soil water distribution was compared to soil moisture measurements recorded with FDR probes. RMSE between observed and calculated soil water content ranged between 0.01 and 0.03 cm^3/cm^3. In the present study RMSE between observed and calculated soil moisture was 0.03 cm^3/cm^3.

Main drawback of the Ψ_{soil} calculation was the poor accordance between calculated and observed Ψ_{soil} in the range between 0 and -20 kPa. Just after irrigation events, or heavy rainfall, the observed Ψ_{soil} increased rapidly to 0 kPa while dryer Ψ_{soil} values were calculated by HYDRUS. The mismatch between observed and calculated Ψ_{soil} can be allocated to the inability of the Watermark sensor to measure matrix potentials higher than the air entry pressure of the sensor which is about -10 kPa (Scanlon et al., 2002). The unreliable Ψ_{soil} observation in the wet range just after rainfall and irrigation

events has previously been observed in similar conditions (Janssens et al., 2011) and can be explained further by hysteresis in the wetting curve from the sensor and failure in dynamic response after partial rewetting of the soil (McCan et al., 1992; Scanlon et al., 2002). In this wet range the calculated Ψ_{soil} probably approximates the true Ψ_{soil} better. This implicates that sensor placement in the wet range of the soil, with Ψ_{soil} above -20 kPa, leads to overestimation of Ψ_{soil}. This increases the risk of inaccurate irrigation scheduling, especially when Ψ_{soil} is maintained close to -30 kPa such as e.g. Janssens et al. (2009) which reflects farmers' practices in Belgium. The Ψ_{soil} calculation in the experiment showed that after irrigation to a rate of 80% ET the wet range of the soil extended to the entire irrigated side of the tree to a depth of 70 cm.

4.2. Sensitivity of the calculation to the selected root distribution

Root length concentrations in the three plots showed a gradual decrease with depth similar to Gong et al. (2006), Besharat et al. (2010), Yao et al. (2011) and others. In the horizontal direction root maximal length densities were observed at 30 and 50 cm distance from the tree trunk. Green and Clothier (1999) showed already for apple that maximal root length concentrations not are necessarily situated close to the trunk. On the contrary root weight concentration, was always higher close to the tree trunk in accordance to coarse root observations in one of the plots. The discrepancy between mass and length of fine roots was previously observed by Oppelt et al. (2005) in tropical fruit tree species.

In the majority of root water uptake studies in fruit trees, the root zone is parameterized based on observed root length distribution (Gong et al., 2006; Green and Clothier, 1999; Green et al., 2003; Yao et al., 2011; Zhou et al., 2007). Only Satchithanantham et al. (2014) expressed recently root distribution in terms of weight distribution by discussing the water uptake of potato. Determining fine root length is slightly more time consuming then achieving fine root weight since roots need to be scanned photographically. For two of the three plots (plot A and B) the quality of the numerical calculation was comparable between calculations based on RLD and RWD. However in one of the three plots (plot C) a satisfying calculation of Ψ_{soil} was only possible using RLD to parameterize the root zone. Furthermore mild water stress in this plot, observed by depressed Ψ_{stem} and altered sap flux density, could not be reproduced by HYDRUS while parameterizing the root zone using RWD. Likewise RLD could be correlated to Ψ_{soil} observations, similar to observations in olive (Searles et al., 2009), while RWD could not. The relationship between RLD and Ψ_{soil} variation was dominated by the observations in the non-irrigated plot C where the highest RLD was observed at the sensors where the lowest Ψ_{soil} was measured. This observation needs to be confirmed by other similar observations but may illustrate how fine root growth is related to water uptake. Previously Green and Clothier (1995) addressed the altered root water uptake patterns in kiwi fruit vine mainly to changes in root distribution. Garré et al. (2011) showed the relation between soil wetting and root growth in a lysimeter. It makes sense that fine root growth is better captured with RLD rather than RWD.

Likewise the calculation of root water uptake using root distributions derived from literature yielded good results in two out of the three plots (plot A and B) it failed in the third plot (plot C). In this case literature root observations were taken from apple orchards (Besharat et al., 2010; Gong et al., 2006) due to the lack of root observations in pear orchards but a similar deficient Ψ_{soil} calculation can be expected when using root observations from other pear tree orchards. The present experiment shows how root distribution is tree specific and that it has significant impact on the numerical calculation of Ψ_{soil}.

5. Conclusion

With the present experiment it was shown how Ψ_{soil} observations measured with Watermark sensors agreed reasonably with numerically calculated Ψ_{soil}. Only when observed Ψ_{soil} increased above -20 kPa the observed Ψ_{soil} did not correspond with the calculated Ψ_{soil}, possibly due to the limitations of the Watermark sensors to measure Ψ_{soil} in the wet range, above -20 kPa. This suggests that positioning sensors close to the irrigation drippers should be avoided to prevent overestimation of Ψ_{soil} and inaccurate irrigation scheduling. In the present experiment this wetting front in the soil, with Ψ_{soil} above -20 kPa, extended to a depth of 70 cm on the entire irrigated side of the tree when irrigation was applied to a rate of 80% ET. The wetting front remained concentrated around the drippers when irrigation was applied to a rate of 50% ET. Furthermore it was shown how site specific observations of RLD are preferred to parameterize the root zone for a reliably calculation of Ψ_{soil}. The Ψ_{soil} calculation with the root distribution parameterized by RLD gave satisfactory results for all plots, while a Ψ_{soil} calculation based on other root observations did not. It evidences that root zone parameterization has a significant influence on the Ψ_{soil} calculation in pear orchards.

Acknowledgments

References

Allen, R.G., Pereira, L.S., Raes, D., Smith, M., 1998. Crop Evapotranspiration. Guidelines for Computing Crop Water Requirements. FAO, Rome (Irrigation and drainage paper).

Arbat, G., Puig-Bargues, J., Barragan, J., Bonany, J., Ramirez de Cartegena, F., 2008. Monitoring soil water status for micro-irrigation management versus modelling approach. Biosyst. Eng. 100, 286–296.

Besharat, S., Nazemi, A.H., Sadraddini, A.A., 2010. Parametric modeling of root length density and root water uptake in unsaturated soil. Turk. J. Agric. For. 34, 439–449.

Bourget, S.J., Elrick, D.E., Tanner, C.B., 1958. Electrical resistance units for moisture measurements:their moisture hysteresis uniformity and sensitivity. Soil Sci. 86, 298–304.

Consoli, S., Stagno, F., Roccuzzo, G., Cirelli, G.L., Intrigliolo, F., 2014. Sustainable management of limited water resources in a young orange orchard. Agric. Water Manag. 132, 60–68.

Dupuy, L., 2003. Modélisation de L'ancrage Racinaire des Arbres Forestiers. Université de Bordeaux I, France (Ph.D. thesis).

Feddes, R.A., Kowalik, P.J., Zaradny, H., 1978. Simulation of Field Water Use and Crop Yield. John Wiley & Sons, New York.

Fernandez, J.E., Green, S.R., Caspari, H.W., Diaz-Espejo, A., Cuevas, M.V., 2008. The use of sap flow measurements for scheduling irrigation in olive, apple and Asian pear trees and in grapevines. Plant Soil 305, 91–104.

Garré, S., Javaux, M., Vanderborght, J., Pagès, L., Vereecken, H., 2011. 3D electrical resistivity tomography to monitor root zone water dynamics. Vadose Zone J. 10, 412–421.

Girona, J., Marsal, J., Mata, M., Del Campo, J., 2004. Pear crop coefficients obtained in a large weighing lysimeter. Acta. Hortic. (ISHS) 664, 277–281.

Godin, C., Caraglio, Y., 1998. A multiscale model for plant topological structures. J. Theor. Biol. 191, 1–46.

Gong, D., Kang, S., Zhang, L., Taisheng, D., Yao, L., 2006. A two-dimensional model of root water uptake for single apple trees and its verification with sap flow and soil content measurements. Agric. Water. Manag. 83, 119–129.

Gonzalez-Altozano, P., Pavel, E.W., Oncins, J.A., Doltra, J., Cohen, M., Paço, T., Massai, R., Castel, J.R., 2008. Comparative assessment of five methods of determing sap flow in peach trees. Agric. Water Mang. 95, 503–515.

Granier, A., 1985. Une nouvelle méthode pour la mesure du flux de sève brute dans le tronc des arbres. Ann. Sci. For. 42, 193–200.

Green, S.R., Clothier, B., 1995. Root water uptake by kiwifruit vines following partial wetting of the root zone. Plant Soil 173, 317–328.

Green, S.R., Clothier, B., 1999. The root zone dynamics of water uptake by a mature apple tree. Plant Soil 206, 61–77.

Green, S.R., Vogeler, I., Clothier, B.E., Mills, T.M., Van Den Dijssel, C., 2003. Modelling water uptake by a mature apple tree. Aust. J. Soil. Res. 41, 365–380.

Jabro, J.D., Evans, R.G., Kim, Y., Iversen, W.M., 2009. Estimating in situ soil–water retention and field water capacity in two contrasting soil textures. Irrig. Sci. 27, 223–229.

Janssens, P., Elsen, F., Vandendriessche, H., Deckers, T., Schoofs, H., Verjans, W., 2009. Effects of regulated deficit irrigaiton on pear trees 'Conference' under temperate zone climate. Acta Hortic. (ISHS) 889, 281–289.

Janssens, P., Deckers, T., Elsen, F., Elsen, A., Schoofs, H., Verjans, W., Vandendriessche, H., 2011. Sensitivity of root pruned 'Conference' pear to water deficit in a temperate climate. Agric. Water. Manag. 99, 58–66.

Kessler, J., Oosterbaan, R.J., 1974. Determining hydraulic conductivity of soils. In: de Ridder, N.A., Takes, C.A.P., van Someran, C.L., Bos, M.G., Messemaekers, Van de Graaf, R.H., Bokkers, A.H.F. (Eds.), Drainage Principles and Applications International Institute for Land Reclamation & Improvement. Wageningen, The Netherlands, pp. 292–294.

Kool, J.B., Parker, J.C., 1987. Development and evaluation of closed-form expressions for hystereticsoil hydraulic properties. Water Resour. Res. 23, 105–114.

Lamari, L., 2002. ASSESS: Image Analysis Software for Plant Disease Quantification. The American Phytopathological Society Press, St. Paul, MN.

Leib, B.G., Jabro, J.D., Matthews, G.R., 2003. Field evaluation and performance comparison of soil moisture sensors. Soil Sci. 168, 396–408.

McCan, I.R., Kincaid, D.C., Wang, D., 1992. Operational characteristics of the watermark model 200 soil water potential sensor for irrigation management. Appl. Eng. Agric. 8, 603–609.

Nolz, R., Kammerer, G., Cepuder, P., 2013. Calibrating soil water potential sensors integrated into a wireless monitoring network. Agric. Water Manag. 116, 20–21.

Oppelt, A.L., Kurth, W., Jentschke, G., Gobold, D.L., 2005. Contrasting rooting patterns of some arid-zone fruit tree species from Botswana–I Fine root distribution. Agrofor. Syst. 64, 1–11.

Phogat, V., Mahadevan, M., Skewes, M., Cox, J., 2012. Modelling soil water and salt dynamics under pulsed and continuous surface drip irrigation of almond and implications of system design. Irrig. Sci. 30, 315–333.

Pradal, C., Boudon, F., Nouguier, C., Chopard, J., Godin, C., 2009. PlantGL: a python-based geometric library for 3D plant modeling at different scales. Gr. Models 71, 1–21.

Rocha, D., Abbasi, F., Feyen, J., 2006. Sensitivity analysis of soil hydraulic properties on subsurface water flow in furrows. J. Irrig. Drain. Eng. 132, 418–424.

Satchithanantham, S., Krahn, V., Sri Ranjan, R., Sager, S., 2014. Shallow groundwater uptake and irrigation water redistribution within the potato root zone. Agric. Water Manag. 132, 101–110.

Scanlon, B.R., Andraski, B.J., Bilskie, J., 2002. Miscellaneous methods for measuring matric or water potential. In: Dane, J.H., Topp, G.C. (Eds.), Methods of Soil Analysis, Part 4, Physical Methods. Soil Science Society of America, Inc., Madison, pp. 643–670 (No. 5).

Schaap, M.G., Leij, F.J., Van Genuchten, M.T., 2001. ROSETTA: a computer program for estimating soil hydraulic properties with hierarchical pedotransfer functions. J. Hydrol. 251, 163–176.

Scholander, P.F., Hammel, H.T., Bradstreet, E.D., Hemmingsen, E.A., 1965. Sap pressure in vascular plants. Science 148, 339–346.

Searles, P.S., Saravia, D.A., Rousseaux, C., 2009. Root length density and soil water distribution in drip-irrigated olive orchards in Argentina under arid conditions. Crop Pasture Sci. 60, 280–288.

Simunek, J., Van Genuchten, M.T., Sejna, M., 2006. The HYDRUS Software Package for Simulating Two- and Three-dimensional Movement of Water, Heat, and Multiple Solutes in Variably-saturated Media, Technical Manual, Version 1.0, PC Progress, Prague, Czech Republic.

Skaggs, T.H., Trout, T.J., Simunek, J., Shouse, P.J., 2004. Comparison of HYDRUS-2D simulations of drip irrigation with experimental observations. J. Irrig. Drain. Eng. 130, 304–310.

Steppe, K., De Pauw, D.J.W., Lemeur, R., 2008. A step towards new irrigation scheduling strategies using plant-based measurements and mathematical modeling. Irrig. Sci. 26, 505–517.

Thompson, R.B., Gallardo, M., Aguera, T., Valdez, L.C., Fernandez, M.D., 2006. Evaluation of the watermark sensor for use with drip irrigated vegetable crops. Irrig. Sci. 24, 185–202.

Van Genuchten, M.T., 1980. A closed-form equation for predicting the hydraulic conductivity of unsaturated soils. Soil. Sci. Soc. Am. J. 44, 892–898.

Vrugt, J.A., Hopmans, J.W., Simunek, J., 2001 a. Calibration of a two-dimensional root water uptake model. Soil Sci. Soc. Am. J 65, 1027–1037.

Vrugt, J.A., Van Wijk, M.T., Hopmans, J.W., Simunek, J., 2001 b. One-, two-, and three-dimensional root water uptake functions for transient modeling. Water Resour. Res. 37, 2457–2470.

Whaylley, W.R., Watts, C.W., Hilhorst, M.A., Bird, R.A., Balendonck, J., Longstaff, D.J., 2001. The design of porous material sensors to measure the matric potential of water in soil. Eur. J. Soil Sci. 52, 511–519.

Yao, P., Dong, X., Hu, A., 2011. Using HYDRUS-2D simulate soil water dynamic in jujube root zone under drip irrigation. ISWREP, 684–688.

Zhou, Q., Kang, S., Zhang, L., Li, F., 2007. Comparison of APRI and Hydrus-2D models to simulate soil water dynamics in a vineyard under alternate partial root zone drip irrigation. Plant Soil 291, 211–223.